

Contents list available at CBIORE journal website

F RE International Journal of Renewable Energy Development

Journal homepage: https://ijred.cbiore.id



Research Article

Starch – carrageenan based low-cost membrane permeability characteristic and its application for yeast microbial fuel cells

Marcelinus Christwardana^{a,b*}, Satrio Kuntolaksono^o, Athanasia Amanda Septevani^{d,e}, H. Hadiyanto^f

Abstract. Microbial fuel cells (MFCs) are an innovative method that generates sustainable electricity by exploiting the metabolic processes of microorganisms. The membrane that divides the anode and cathode chambers is an important component of MFCs. Commercially available membranes, such as Nafion, are both costly, not sustainable, and harmful to the environment. In this study, a low-cost alternative membrane for MFCs based on a starch-carrageenan blend (SCB-LCM) was synthesized. The SCB-LCM membrane was created by combining starch and carrageenan and demonstrated a high dehydration rate of 98.87 % over six hours. SEM analysis revealed a smooth surface morphology with no pores on the membrane surface. The performance of SCB-LCM membrane-based MFCs was evaluated and compared to that of other membranes, including Nafion 117 and Nafion 212. All membranes tested over 25 hours lost significant weight, with SCB-LCM losing the least. The maximum power density (MPD) of the SCB-LCM MFCs was 15.77 ± 4.34 mW/m², indicating comparable performance to commercial membranes. Moreover, the cost-to-power ratio for MFCs employing SCB-LCM was the lowest (0.03 USD.m²/mW) when compared to other membranes, indicating that SCB-LCM might be a viable and cost-effective alternative to Nafion in MFCs. These SCB-LCM findings lay the groundwork for future research into low-cost and sustainable membrane for MFC technologies.

Keywords: Biomass; Bioenergy; Energy Production; Renewable Energy; Sustainable Energy



@ The author(s). Published by CBIORE. This is an open access article under the CC BY-SA license (http://creativecommons.org/licenses/by-sa/4.0/). Received: 26th Oct 2023; Revised: 15th January 2024; Accepted: 17th Feb 2024; Available online: 25th Feb 2024

1. Introduction

Nowadays, over 90% of energy is created using fossil fuels (coal, natural gas, and petroleum), and around 10% is generated from renewable energy sources (Maity *et al.*, 2014). The energy produced by fossil fuels is neither renewable nor sufficiently abundant to fulfill the world's expanding energy needs (Wang *et al.*, 2014). Additionally, energy production process contributes to the greenhouse gases emission that contribute to global warming and environmental damage (Tebaldi *et al*, 2021). By 2042, fossil fuels are expected to be depleted (Mohr *et al*, 2021). Consequently, an immediate requirement exists for the creation of a novel renewable energy source, exemplified by biodiesel (Ahmed, 2015), bioethanol (Tse *et al.*, 2021), and also hydrogen fuel cells (Singla *et al.*, 2021).

Recently, the microbial fuel cell (MFC) has been hailed as an exciting future alternative, a novel technology, and a source of renewable and green energy (Cheng *et al.*, 2014; He *et al.*, 2017; Arun *et al.*, 2024), and it has been rapidly evolving over the last several decades (Boas *et al.*, 2022; Maddalwar *et al.*, 2021). MFCs are bio-electrochemical devices that transform chemical

energy contained in organic/inorganic substrates (Kumar et al., 2015) to electrical energy through electrochemical processes (Ghasemi & Rezk, 2024; Zhang et al., 2020) and microbe activity (Senthilkumar et al., 2020; Hadiyanto et al., 2023). MFC is an eco-friendly technology since it utilizes organic material such as wastewater and provides a dual advantage of bioelectricity production and waste management (Idris et al., 2016; Obileke et al., 2021; Xu et al., 2017). Generally, there are five benefits that enhance the sustainability of MFCs in wastewater treatment: (1) the direct conversion of substrate energy into electricity, (2) reduced sludge production compared to anaerobic digesters and aerobic activated sludge processes, (3) operational resilience even in low-temperature environments, (4) elimination of gas treatment and aeration energy input, and (5) versatile application in areas with inadequate electricity supply. On the other hand, MFC eliminates or significantly reduces the need for aeration (energy savings) (Kumar et al., 2016), the ability to recover valuable products from wastewater, such as electricity (Rabaey & Verstraete, 2005; Zhang et al., 2019; Hadiyanto et al., 2022) and nutrients (Do et al., 2018; Yang et al., 2018), the use of clean and efficient technology (Jatoi et al.,

^aDepartment of Chemistry, Diponegoro University, Jl. Prof. Sudharto, SH, Tembalang, Semarang 50275, Indonesia

^bMaster Program of Energy, School of Postgraduate Studies, Jl. Imam Bardjo, SH, Pleburan, Semarang 50241, Indonesia

^cDepartment of Chemical Engineering, Institut Teknologi Indonesia, Jl. Raya Puspiptek Serpong, South Tangerang 15314, Indonesia

^aResearch Center for Environmental and Clean Technology, National Research and Innovation Agency, KST BRIN Cisitu, Bandung 40135, Indonesia

^eCollaborative Researh Center for Zero Waste and Sustainability, Universitas Katolik Widya Mandala, Surabaya 60114, Indonesia

^fCenter of Biomass and Renewable Energy (CBIORE), Chemical Engineering Department, Diponegoro University, Indonesia

^{*} Corresponding author

2021; Paucar & Sato, 2021a), and the absence of harmful toxic by-products (Jatoi *et al.*, 2021).

Within a MFC, electrons travel from the anodic chamber to the anode electrode and subsequently flow to the cathode through an external circuit. Simultaneously, protons move from the anode to the cathode through a separator commonly known as a membrane or proton exchange membrane (PEM) (Shabani et al., 2020; Sirajudeen et al., 2021). The separator or membrane plays a crucial role in MFCs by physically dividing the anode and cathode chambers, facilitating the movement of cations to the cathode, and thereby sustaining an electrical current (Kim et al., 2007; Vishwanathan, 2021). Key features and functions of membranes in MFCs encompass the separation of anode and cathode chambers, prevention of oxygen back diffusion to the anode, reduction of substrate flux from anode to cathode, enhancement of coulombic efficiency (CE) through minimizing oxygen flux from cathode to the solution in the anode chamber and ensuring effective and enduring operation. Over the past decade, MFC research has explored various membrane types, including cation exchange membranes (CEM), anion exchange membranes (AEM), bipolar membranes (BPM), microfiltration membranes (MFM), ultrafiltration membranes (UFM), glass fibers, porous fabrics, and other coarse pore filter materials. Canvas (Zhuang et al., 2009), carbon paper (Sonawane et al., 2019), nylon-infused membrane (Hernández-Fernández et al., 2015), microporous filtration membranes (Paucar & Sato, 2021b), UltrexTM (Moharir & Tembhurkar, 2018), ceramics (Winfield et al., 2016), and Nafion® (NF) 117 (Chakraborty et al., 2020; Yu et al., 2015) are also examples of PEM. NF 117 type is the most often employed PEM in MFC because of its protonpermeable selectivity, capacity to facilitate ion transfer, and good ionic conductivity (Guo Kun et al., 2012). Conversely, nanofiltration (NF) membranes present several drawbacks such as cathode-to-anode oxygen leakage, water permeability, crossover, and substantial cost (Idris et al., 2016) (costs up to \$1400/m² and the updated price is approximately \$1733/m²) (Xia et al., 2013), which has a significant impact on the overall production cost of MFC in field applications (Hernández-Flores et al., 2015).

Among the several membrane materials, starch is one of the most recently used materials in the MFC area for membrane separators. Starch has garnered substantial interest owing to its unique qualities, the most notable of which are its abundance, renewable nature, low cost, environmental friendliness (biodegradable), and cytocompatibility (Bertuzzi et al., 2007; Talja et al., 2007; Zhong et al., 2020). Additionally, starch, which contains around 30% amylase, 70% amylopectin, and less than 1% lipids and proteins from plants, is an ideal addition for membrane formation due to its insoluble nature (F. Liu et al., 2009). However, starch has a number of disadvantages, including poor physical characteristics (Abdou & Sorour, 2014), a high degree of hydrophilicity, and poor mechanical capabilities when compared to typical synthetic polymers (Ahmed et al, 2020). Carrageenan, a water-soluble polymer composed of partly sulphated galactans, has been suggested to increase the characteristics of starch and is therefore likely to be employed as a film-forming material (Sandhu et al., 2020). Carrageenan is a group of sulphated linear polysaccharides found in the cell walls and intercellular matrix of a variety of red seaweed species (Sandhu et al., 2020). Carrageenan is frequently used in the food industry in a variety of products due to its gelling, stabilizing, and thickening properties, as well as its capacity to form thermo-reversible gels (Castaño et al., 2017). The combination of starch and carrageenan is utilized to create biofilms that have a number of benefits over those created using synthetic material (Castaño *et al.*, 2014; Galus & Kadzińska, 2016)

At the moment, researchers are focused on replacing and decreasing the cost of NF membranes via the use of innovative alternative materials. Sulphonated polyether ketone (SPEEK) was created for usage in MFC (Ayyaru & Dharmalingam, 2011). Their setup achieved peak volumetric powers of 5.7 and 3.2 W/m³ using influents of wastewater and residential wastewater, respectively. In the comparison with NF, the SPEEK membrane demonstrated a power density of approximately 55% higher. Nonetheless, the prohibitive cost of the SPEEK membrane remains a challenge (Galus & Kadzińska, 2016). Additionally, agar was used to create a low-cost organic membrane (LCM), which is a viable option for usage as separators in MFC (Hernández-Flores, et al., 2015). The maximum power density (MPD) of LCM and NF were 2146 and 14246 mW/m², respectively. The MPD delivered by LCM was 15% of that supplied by NF. The cost ratio of LCM to NF was 0.8 % (\$14/m²)/(\$1733/m²). These findings indicate a trade-off between some loss of cell power (85%) and exceptional cost reductions (99.2 %) on membranes (Hernández-Flores, et al., 2015). Additionally, the nonwoven fabric Polypropylene (PP80) may be used as a substitute. The highest voltage of 0.477 V (with 1000Ω) was comparable to NF (0.481 V). The MPD of PP80 and NF were 121 mW/m² and 118 mW/m², respectively. PP80 had a material cost ratio of 0.57 \$/m², whereas NF had a material cost ratio of 2300 \$/m² (Kondaveeti et al., 2014). The research conducted has indeed demonstrated commendable performance in MFCs. However, it is worth noting that the production costs remain relatively high, presenting a challenge for broader-scale applications. This cost consideration suggests that further exploration and optimization may be needed to enhance the suitability of these technologies for larger-scale implementation.

This research aims to showcase the efficacy of a membrane composed of starch and carrageenan in Microbial Fuel Cells (MFCs). Until far, no researcher has used starch carrageenan as a membrane material in MFC applications, so this is an academic novelty in this research. This study performed a thorough examination, comparing the starch-carrageenan membrane to commercially available Nafion® (NF) membranes in terms of their structure, performance, electrochemical properties, and economic factors. The development of affordable membranes has significant relevance not only in the scientific field but also for society and industry. Within the larger framework of society, the endeavor to find membrane solutions that are economical corresponds with objectives related to sustainability, hence enhancing the availability and affordability of clean energy technology. The results of this research have the potential to advance economic efficiency, scalability, and environmental sustainability in industries focused on renewable energy and microbial fuel cell applications. This could lead to the development of more practical and widely adopted clean energy solutions.

2. Materials and method

2.1 Low-Cost Membrane Preparation

Modifications were made to the method described in previous studies (Christwardana et al., 2021; Christwardana, Ismojo, et al., 2022) in order to produce membranes at a reasonable cost or Low Cost Membrane (LCM). Cassava starch (Dwilab Mandiri, Bandung, Indonesia) was added to 60 mL of distilled water, followed by 60 seconds of stirring. Following the addition of 5 mL of glycerol (≥99.0%, Sigma Aldrich, St. Louis, USA), the

mixture was stirred for 60 seconds. The 5% v/v acetic acid (98%, ROFA Laboratory Center, Bandung, Indonesia) was then added to the solution and agitated for an additional 60 s. This process involved heating and stirring for ten minutes at 60 °C. Following the cessation of heating, an additional 60 s of stirring were carried out to minimize foam formation. The resulting solution was then applied to the glass mold's surface and subjected to a seven-day oven-drying period at 30 °C. The outcome was a bioplastic membrane derived from starch known as a starch-based low-cost membrane (SB-LCM). Conversely, a starch-carrageenan-based low-cost membrane (SCB-LCM) was produced using the same procedure with the addition of 1 g of carrageenan (≥95.0%, Research Products International Corp., Illinois, USA) to the mixture.

2.2 Membrane water uptake and permeability analysis

For the liquid-vapor permeability assessments, the solutions examined were distilled water (DW) or a broth solution (BS) consisting of Yeast extract, Peptone, D-glucose (YPD) medium with active yeast. The testing methodology for liquid-vapor permeability, along with calculations for water flux, permeance, and dry/wet water absorption, drew upon existing literature (Liu & Logan, 2004; Vishwanathan, 2021). To conduct the tests, 10 mL of the chosen liquid (DW or BS) was placed in a plastic vial, with a low-cost membrane sample—either Nafion 212 or Nafion 117—interposed between the vial and the cap. The pervaporation area was defined by a 5 mm diameter hole, its perimeter sealed with polymer tape, and the cap secured with parafilm. The vial's bottom featured an aperture for internal/external pressure equilibration. Each sample and liquid underwent duplicate testing to ensure reproducibility. The inverted vials were positioned in a controlled environment, and water loss was measured using a precision scale every 60 minutes over a 24-hour period (Frattini et al., 2020). The total uptake (Utot), wet uptake (Uwet), and dry uptake (Udry) of all membrane samples were computed as follows:

$$U_{tot} = \frac{m_i - m_w}{m_i} \times 100 \tag{1}$$

$$U_{dry} = \frac{m_i - m_d}{m_i} \times 100 \tag{2}$$

$$U_{wet} = U_{tot} - U_{dry} \tag{3}$$

In the given equations, m_i represents the initial dry weight of the samples, m_w is the final weight of the samples following a 24-hour soaking period, and m_d signifies the dried weight of the samples after 24 hours of testing and subsequent vacuum drying to eliminate all traces of water, leaving only the solid residue representing the biofilm. The net water intake, Uwet, is calculated as the disparity between total and dry uptake, as expressed in equation (3). The permeability experiments were conducted at a temperature of 27 °C (300 K) and a relative humidity (RH) of 50%. To account for this, slight adjustments to the chemical potentials were necessary, as per the following equations (4) for water flux, chemical potentials, and permeance (Adachi *et al.*, 2010).

$$J_{LVP} = \frac{(m_{tn} - m_{tn-1}) \times 60 \times 1000}{(PM_{H2O} \times A_{LVP} \times \Delta t) \times 3.6}$$
(4)

In the provided context, J_{LVP} denotes the molar liquid-vapor permeation flow (mol.m⁻².s⁻¹), m_{tn} and m_{tn+1} represent the relative weight losses (g) at tn and tn+1, PM_{H2O} stands for the molecular weight of water (18.015 g mol⁻¹), ALVP signifies the

exposed pervaporation area (mm²), and t corresponds to the time period (60 min) between tn and t_{n+1} .

2.3 Electrochemical measurement

The acrylic single-chamber Microbial Fuel Cell (MFC) reactor, procured from Phychemi Co. Ltd. (Beijing, China), was employed in the conducted experiment. The anode chamber was filled with a 28-ml anolyte comprising fresh YPD medium, consisting of 2.5 mg/mL of peptone (Himedia, Mumbai, India), 5 mg/mL of yeast extract (Merck, Darmstadt, Germany), and 14 mg/mL of D-glucose (Merck, Darmstadt, Germany) as a substrate. Additionally, 14 mg/mL yeast Saccharomyces cerevisiae served as the biocatalyst (Christwardana et al., 2022, 2023). The cathode was exposed directly to ambient air, with the membrane separator being treated NF (treated with 3% w/w H₂O₂, 0.5M H₂SO₄, and DI water). The plain carbon felt (CF) was utilized as both an anode and a cathode, possessing a projected surface area of 7 cm², appropriately positioned in their respective locations. A stainless-steel wire functioned as the current collector, and the experiment was conducted in an open-air setting at a temperature of approximately 25 °C. The crucial parameters for assessing the MFC's performance were voltage and power density. For voltage measurement, a UNI-T UT61E multimeter (Dongguan, China) and a 1000 Ω external load were employed in conjunction with the MFC reactor. The output voltage was recorded every 15 minutes using a datacollecting device over a 48-hour period (Christwardana et al., 2022). To determine the MFC discharge power density, loads ranging from 5 M Ω to 10 Ω (Elenco RS500 Resistance Substitution Box, Illinois, USA) were applied between the anode and the cathode. The current density (J) was calculated by dividing the voltage by the resistance and the anode's projected surface area. The maximum power density (MPD) was obtained by multiplying the current density by the voltage. Each measurement was repeated three times, and the average with its standard deviation was recorded.

2.4 Dehydration and SEM Analysis

The membrane weight during the drying process is monitored hourly to obtain a value indicating the dehydration of the low-cost membrane. The percentage dehydration is calculated by taking the difference between the initial weight and the weight at time t, dividing it by the initial weight, and then multiplying by 100%. The surface morphology of the low-cost membranes was examined using a scanning electron microscope, specifically the FEI Inspect F50 (Oregon, USA), in a high vacuum environment.

2.5 Techno-economic Analysis

In the techno-economic analysis, the evaluation included the calculation and analysis of membrane costs within the system. Additionally, the examination of the power-to-cost ratio and cost-to-power ratio provided a comprehensive understanding of the economic feasibility and efficiency of the developed technology. This thorough assessment of techno-economic factors contributes valuable insights into the economic implications and viability of the membrane-based system for MFCs.

3. Results and Discussion

3.1 Chemical Interaction in LCM

In the realm of membrane technology, the interaction between different types of membranes plays a crucial role in

Fig. 1 Structure of SB-LCM and SCB-LCM

determining their overall performance and applicability. In this context, interactions between two distinct kinds of membranes: SB-LCM and SCB-LCM, based on their chemical structure was delved into the thermodynamic and shown in Figure 1.

Starch is constructed from glucose units linked by α -1,4 and α-1,6 glycosidic bonds (Cui et al., 2021). The glucose units in starch repeat and contain hydroxyl (-OH) groups, imparting high polarity and the ability to form hydrogen bonds, particularly with water molecules (Xu & Shi, 2019). Upon contact with an aqueous environment, SB-LCM engages in hydrogen bonding between the hydroxyl groups and water molecules (B. Liu et al., 2020). This interaction results in membrane swelling as water is absorbed into the polymer matrix. The swelling behavior of starch-based membranes is important to consider in practical applications. While it can enhance the membrane's permeability to some solutes, excessive swelling might compromise the membrane's mechanical stability and long-term performance (Cui et al., 2021). Thus, controlling the degree of swelling becomes a critical aspect of designing starch-based membranes for specific separation processes.

Carrageenan consists of repeating galactose units, some of which are sulfate groups (Guo et al., 2022). These sulfate groups introduce additional charged sites on the carrageenan molecule, making it more hydrophilic and capable of forming even stronger hydrogen bonds with water and other polar solutes (Shrgawi et al., 2023). When starch and carrageenan are combined to create an SCB-LCM, their respective interactions with water and other solutes create a complex thermodynamic environment. Both starch and carrageenan contain numerous hydroxyl (-OH) groups in their molecular structures. The polar hydroxyl groups possess the ability to establish hydrogen bonds

with each other. Hydrogen bonding, a robust and specific interaction, occurs between the hydrogen atom of one hydroxyl group and the oxygen atom of another hydroxyl group. The existence of hydrogen bonding between starch and carrageenan molecules enhances their mutual solubility and compatibility, enabling the formation of a blend or mix-based membrane. The hydrogen bonding ability of both starch and carrageenan is amplified in the mix-based membrane, resulting in enhanced hydrophilicity and affinity for water-based solutions. This increased hydrophilicity may lead to further swelling of the mixbased membrane compared to the pure starch-based membrane. Carrageenan contains negative sulfate groups in its molecular structure, while the hydroxyl groups in starch are generally uncharged (Qureshi et al., 2019). The difference in charge generates electrostatic interactions between the positively charged hydrogen atoms in starch and the negatively charged sulfate groups in carrageenan. These electrostatic interactions serve to reinforce the binding between starch and carrageenan, thereby augmenting their compatibility in a mixbased membrane. The combination of hydrogen bonding and electrostatic interactions allows starch and carrageenan to create a cohesive structure when blended together, resulting in a stable and functional mix-based membrane. This blend of two different polysaccharides with complementary properties offers better selectivity compared to starch-based membranes.

3.2 Physical characterization of the low-cost membrane

The membrane dehydration mechanism and the membrane thickness are crucial to the analysis. This procedure resulted in a dehydration rate of 98.34 \pm 0.06 percent over five hours of SB-LCM, while the dehydration rate of SCB-LCM, as seen in Figure 2a, was 98.87 \pm 0.07 % over six hours. The water evaporated on

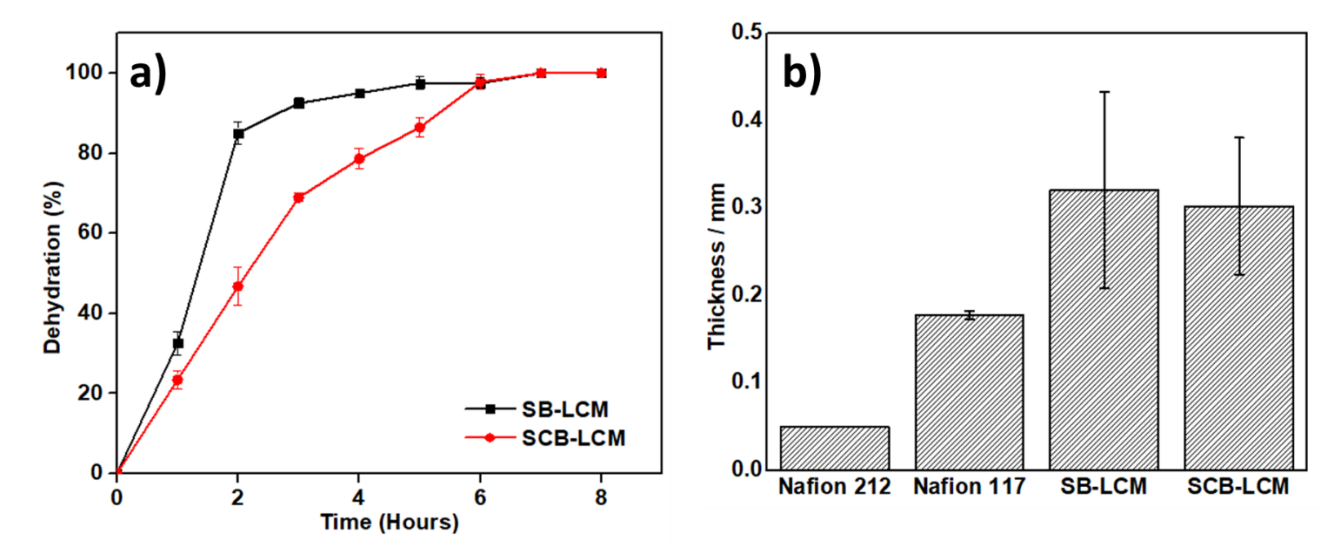


Fig. 2 a) Dehydration of SB-LCM and SCB-LCM over the time, while b) is the thickness of commercial and synthesized membrane

SB-LCM one hour faster than SCB-LCM is likely due to SB-LCM having more pores. An abundance of pores might have negative consequences when used as an MFC separator. This occurs because the electrolyte solution in the anode chamber has the ability to pass through the holes of the membrane and leak into the opposite side, known as the cathode side, which is not desirable. The dehydration time in SB-LCM is comparable to the LCM dehydration time carried out by several previous researchers where the average dehydration time was 5-6 hours (Hernández-Flores $\it et al., 2015a; Hernández-Flores, \it et al., 2015b).$ The dry membrane thicknesses for SB-LCM and SCB-LCM have been respectively 0.321 \pm 0.122 mm and 0.302 \pm 0.078 mm as shown in Figure 2b. The thicknesses measured were 0.053 \pm 0.000 mm and 0.177 \pm 0.005 mm respectively, as regards the commercial membranes of the Nafion 212 and 117.

SEM photographs are used to demonstrate the evaporation analysis in the previous section as seen in Figure 3. Figure 3a is a SEM image of the SB-LCM, in which the membrane surface has several pores. The pores are high in count, uniform and

around 0.9 µm in dimension. In contrast, no pores have been detected on the surface in SCB-LCM (Figure 3b). The pores on the membrane surface are covered by carrageenan, which makes the process of water evaporation slower. The presence of pores in the SB-LCM is indicative of the membrane's void volume. According to Figure 3b, the empty area is filled with air, which causes the SB-LCM to be somewhat thicker than the SCB-LCM

$3.3\ Permeability\ and\ biofouling\ behavior\ of\ low-cost\ membrane$

For DW and BS, permeability and biofouling tests were prepared with two types of NF: NF 212, NF 117, SB-LCM and SCB-LCM membranes. Weight loss and molar flux values have been reported for each repeated test. DW was used to assess the permeability of the four samples, as in Figure 4a-b. In DIW, owing to the liquid-vapor permeation phenomenon, it transports only water across the sample. In this situation, the inside of a sample contact with the fluid directly, while the outside of the sample was exposed to air, meaning that the fluid eventually

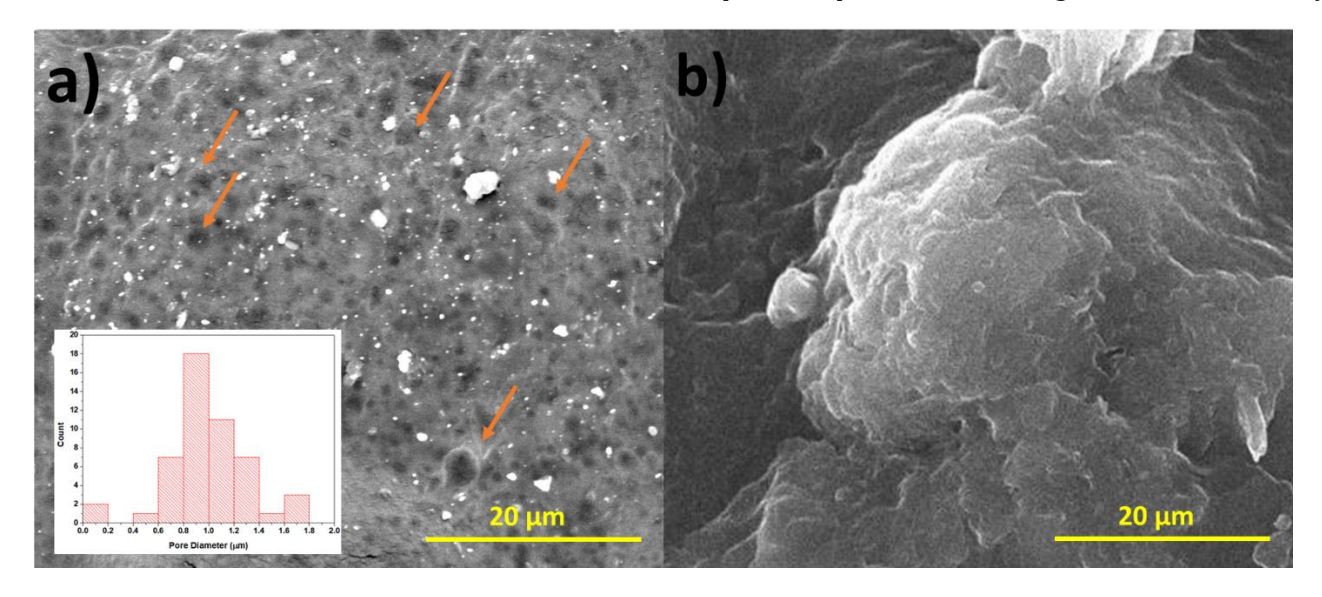


Fig. 3 SEM images of a) SB-LCM and b) SCB-LCM. Inset is pores diameter distribution. Arrows show the pores of membrane

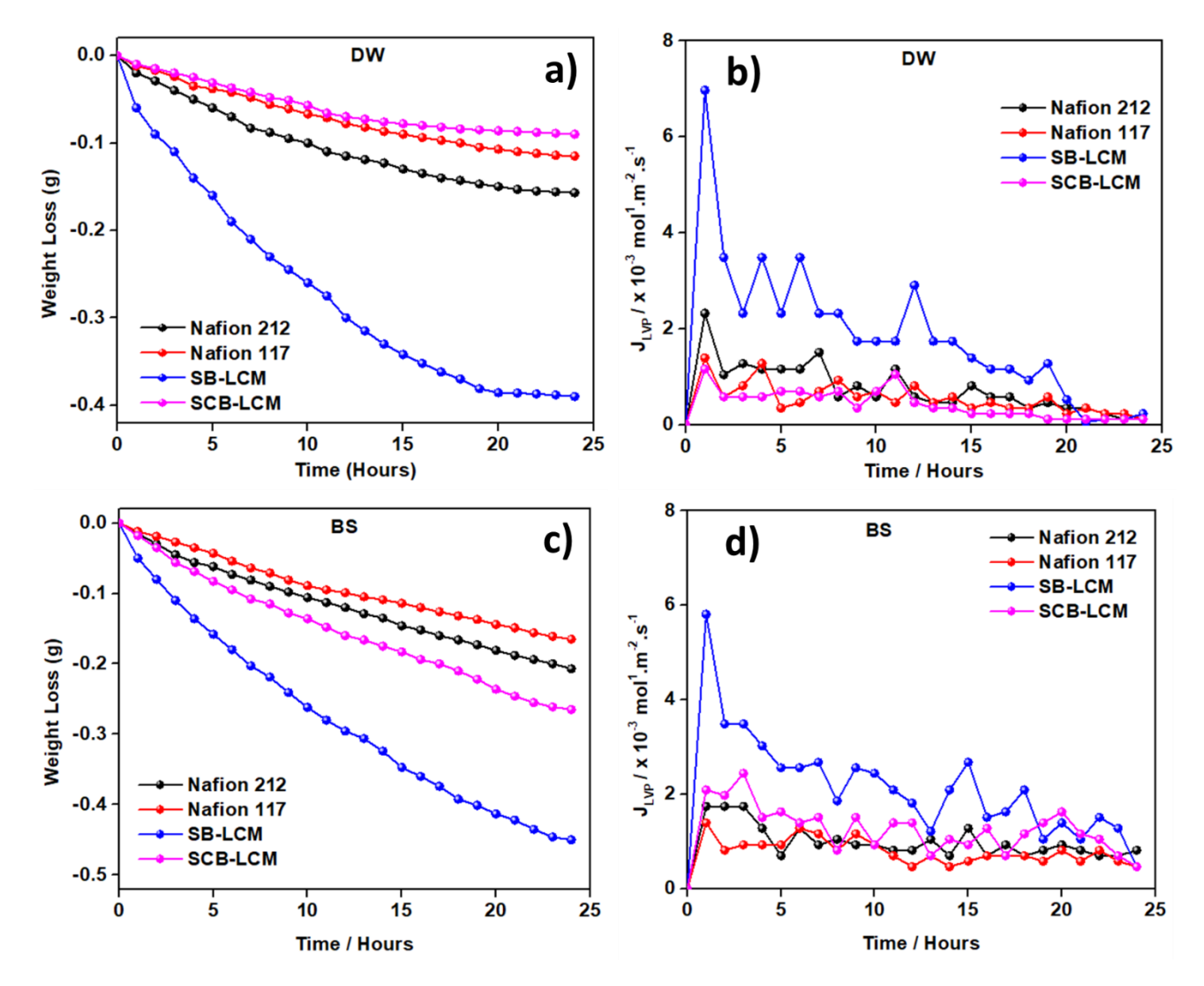


Fig. 4 Permeability results with DW for a) relative weight losses; b) water flux of commercial and synthesized membrane, while (c-d) permeability results with BS

diffused side by side and gradually evaporated into the air. This is due to the discrepancy between the concentration gradient on the sample and the environmental air.

Two low-cost membrane separators exhibit promising weight loss compared to NF 117 and NF 212 in Figure 4a. The weight loss in SB-LCM is higher than SCB-LCM, NF 212, and NF 117 as its porosity is higher so the water evaporates into the air more rapidly. The loss in weight is around -0.390 g in the SB-LCM after 25 hours. SCB-LCM weight loss is lower compared to other membranes as carrageenan closes the pores in the membrane surface. Carrageenan prevents the access and evaporation of water so that the water weight loss has a sluggish rate of -0.090 g and is usually stagnant for 25 hours. A considerable loss of weight on NF 117 was observed which was marginally faster than the SCB-LCM, i.e., -0.115 g in 25 hours. Although NF 212 weight loss was over NF 117 in 25 hours, i.e., -0.157 g.

In the meantime, the water molar flux of the four samples shown in Figure 4b indicates the distinct activity of every specimen. The SB-LCM was hydrated immediately and after 10 hours achieves a nearly steady flow of water, and decreases after the 20th hour. NF 117 shows relatively slow hydration properties, as NF 212, but this isn't overcome entirely, and molar flux flow slightly declines with time and after eight hours

enter an almost steady flow. SCB-LCM has a very sluggish, minimally reduced flux compliance behavior because of the possibility of limited porosity and a much thicker than other samples, which makes water transport longer time.

These phenomena, taken together, are linked to many aspects, such as various porosities and varying wetness of the sample's internal surface that is exposed to the liquid. Hydration is a key step in the transport mechanism in the proton conductive polymer. Concerning the surplus porosity and pore size of the SB-LCM, water transport was described as nearly unrestrained and unpredictable. In contrast, the water transport in the SCB-LCM was more manageable due to the encapsulation of carrageenan within the membrane pores.

When DW was changed to BS, this theory was verified. The permeability test with BS seen in Figure 4c-d was carried out. During the vial test, additional sealing was performed during the use of BS to mitigate the fluid escape. In this case, BS is the medium in MFC that contains an active biocatalyst yeast that alters the glucose substrate to generate protons, electrons, CO_2 gas and additional H_2O (Christwardana *et al.*, 2021). Water flux and weight loss data vary significantly in the presence of BS. As shown in Figure 4c, a considerable loss of weight on NF 117, NF 212, SB-LCM, SCB-LCM were observed i.e., -0.165, -0.207, -0.265, and -0.165 g in 25 hours, respectively. The vial was

Table 1Absolute final and dry uptakes of commercial and synthesized membrane with DW and BS.

| Stage | Nafion 212 | | Nafion 117 | | SB-LCM | | SCB-LCM | |
|---------|------------|---------|------------|---------|------------|---------|------------|---------|
| | Weight (g) | Δwt (g) |
| | | | | DW | | | | |
| Initial | 0.032 | - | 0.080 | - | 0.072 | - | 0.071 | - |
| Final | 0.052 | 0.020 | 0.126 | 0.046 | 0.223 | 0.151 | 0.133 | 0.062 |
| Dry | 0.033 | 0.001 | 0.081 | 0.001 | 0.070 | 0.002 | 0.070 | 0.001 |
| | | | | BS | | | | |
| Initial | 0.031 | - | 0.082 | - | 0.048 | - | 0.102 | - |
| Final | 0.051 | 0.037 | 0.118 | 0.036 | 0.136 | 0.098 | 0.169 | 0.067 |
| Dry | 0.041 | 0.010 | 0.088 | 0.006 | 0.064 | 0.016 | 0.110 | 0.008 |

inverted, positioning the liquid in direct contact with the sample to simulate the most severe biofouling condition. Additional water and CO₂ gas byproducts were produced to create excessive pressure, facilitating the forcing of water and/or gas through the membrane. In cases where the sample exhibits high porosity, large pore diameter, and good wettability, the membrane sample can effectively disperse water. These characteristics in the presence of BS contribute to free percolation and do not facilitate regulated water leaks when real YPD medium and yeast are used in MFC. Based on the information provided earlier, it has been confirmed that SB-LCM is not a suitable material to be used as a separator in a microbial fuel cell (MFC). In contrast, materials such as NF 212, NF 117, and SCB-LCM have demonstrated the ability to withstand high levels of water and CO2 pressure, especially when an external pressure, referred to as BS, is applied to the membrane's inner side. And as the flux rises, the liquid cannot be percolated to the outside membrane.

In particular, where the liquid is transformed from DW into BS, the SCB-LCM has the highest apparent permeability as any other membrane sample (Figure 4d). When tested with BS, the permeance of SB-LCM, NF 212, and NF 117 was almost the same. Therefore, water and gas transport through SB-LCM is more likely to occur under BS than under DW. SCB-LCM is a promising biopolymer separator material for MFC and therefore may be an alternative choice.

Figure 5 compares the relative drawings of the four samples. As expected, the water contribution in DW only absorbs water and is removed after drying almost entirely as shown in Figure 5a. When DW was replaced by BS, the situation was slightly different (Fig. 5b). BS includes dissolved solids and yeast cells that are likely to settle on the membrane and be absorbed in pores and cannot be lost even after washing and drying. The relatively high rate of absorption of SB-LCM and biofouling occurrence was about 29% of total absorption, with a seventh of total absorption of BS from a relative standpoint. The contribution of biofouling to the SCB-LCM membrane is almost a tenth of the total absorption and is somewhat closer to NF 117's performance. In the meanwhile, NF 212 is about half of the overall absorption by the biofouling contribution. This indicates a moderately high resistance to biofouling in the SCB-LCM biopolymer membrane as seen in Table 1.

The rate of water diffusion through the SB-LCM and SCB-LCM is contingent on the extent of swelling and the pathways accessible for water molecules to traverse the interconnected pores and voids within the polymer structure. SB-LCM, being

hydrophilic, feature polar hydroxyl groups in their molecular structure. Upon contact with water, hydrogen bonding ensues between the hydroxyl groups in starch and water molecules. This interaction facilitates water uptake, causing the membrane to swell as it absorbs water (Gao et al., 2021). The swelling of SB-LCM creates pathways for water molecules to diffuse through the polymer matrix. The rate of water diffusion through the SB-LCM depends on the degree of swelling and the available pathways for water molecules to move through the interconnected pores and voids in the polymer structure. In SCB-LCM, water diffusion is influenced by the combined effects of both starch and carrageenan components. As mentioned earlier, carrageenan is highly hydrophilic due to the presence of sulfate groups, which enhance its interaction with water molecules through stronger hydrogen bonding. When water comes into contact with the mix-based membrane, it is readily absorbed by both the starch and carrageenan regions. However, the reduced porosity of the membrane results in lower water uptake and swelling compared to starch-based membranes. Consequently, water diffusion through SCB-LCM is typically slower than in SB-LCM, aligning with the findings depicted in Figure 5. Moreover, the presence of carrageenan also impacts the selectivity of the membrane, potentially influencing the transport of solutes alongside water (Yadav et al., 2022).

The phase change at the membrane-air interface is an important aspect that can influence the performance of membranes, especially in applications where the membrane is exposed to air or gas phases. SB-LCM, being hydrophilic in nature due to the presence of polar hydroxyl groups, tend to interact strongly with water and readily absorb moisture from the surrounding environment. When these membranes are exposed to air or a gas phase, they tend to adsorb water vapor from the air, leading to a phase change from a dry state to a hydrated or swelled state. As the membrane absorbs water vapor from the air, it undergoes swelling, which affects its overall structure and properties. The increase in moisture content at the membrane-air interface can lead to changes in membrane thickness, porosity, and pore size distribution. This, in turn, can influence the permeability of the membrane to different gases and vapors. Moreover, the phase change at the membrane-air interface can impact the selectivity of the membrane towards certain gases. The existence of water molecules at the interface could influence the interaction between the membrane and particular gas molecules, potentially modifying their transport behavior through the membrane. SCB-LCM, is even more hydrophilic than SB-LCM

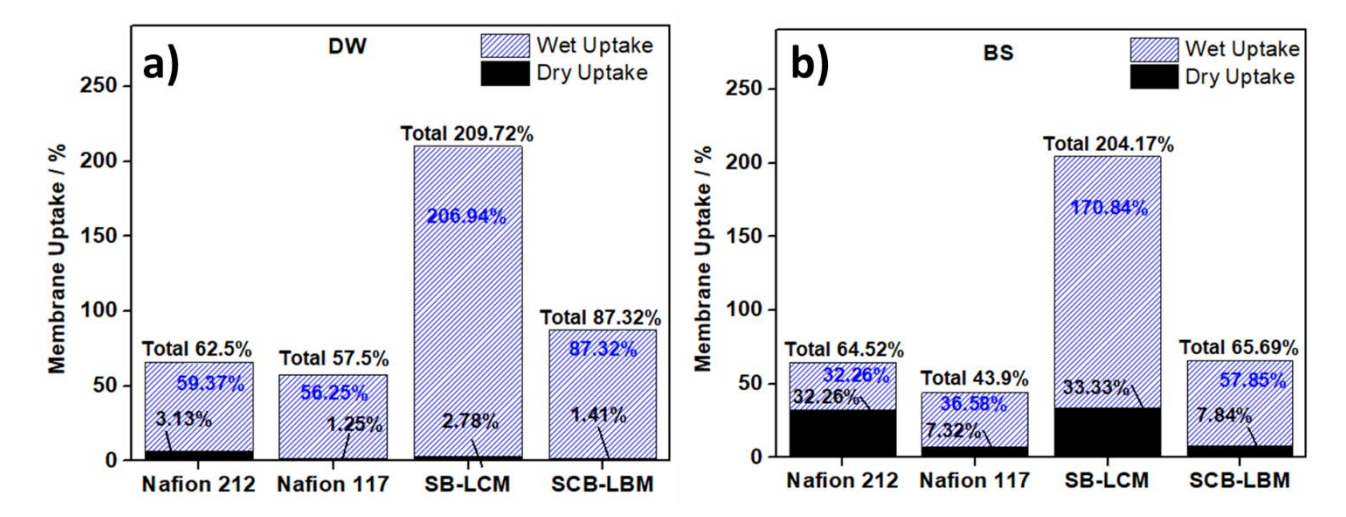


Fig. 5 Relative wet and dry water uptakes of commercial and synthesized membrane with a) DW and b) BS

due to the presence of carrageenan with its sulfate groups. However, the less pores number exhibit decreased moisture uptake when exposed to air or gas phases. Similar to SB-LCM, when the SCB-LCM comes into contact with air or a gas phase containing water vapor, it undergoes a phase change from a dry state to a hydrated or swollen state. The phase change at the SCB-LCM results in insignificant swelling, which can not affect both its structural integrity and gas transport properties. Additionally, the presence of water molecules at the interface may lead to preferential interactions with specific gases, influencing their transport behavior through the membrane (Diawara et al., 2021).

3.4 Electrochemical analysis

The use of a low-cost membrane on a single-cell MFC was investigated, and its performance was evaluated based on its resulted voltage and the MPD. Figure 6a depicts some of the behaviors that can be seen. A similar phenomenon was seen on the voltage curve of the MFC employing NF 117, NF 212, and SCB-LCM. For SB-LCM, the rise in voltage was not too significant from 0 to 42 hours since yeast entered the lag phase (from 0.002 to 0.03 V), but there was a considerable increase in

voltage from 42 to 60 hours as yeast underwent quick growth or entered the logarithmic phase (from 0.03 to 0.06 V). Furthermore, the voltage curves at NF 212 and 117 became stationary, while at SCB-LCM, the voltage dropped owing to a leak in the membrane caused by SCB-LCM absorbing too much anolyte and breaking. In the meanwhile, a similar occurrence occurred in SB-LCM, albeit at a quicker rate. When the membrane was damaged at the 27th hour, the voltage decreased dramatically. This demonstrates that SB-LCM easily absorbs water and reduces the membrane's strength (Christwardana *et al.*, 2021).

Figure 6b demonstrates the MPD values for four different membrane types used in MFCs. The highest MPD was achieved by MFC using NF 117 at 61.74 ± 6.73 mW/m², followed by MFC using NF 212 at 26.84 ± 2.73 mW/m². Meanwhile, MFCs using SCB-LCM achieved MPDs of about 15.77 ± 4.34 mW/m², while MFCs using SB-LCM achieved the lowest MPD of around 6.77 ± 1.24 mW/m². This implies that the usage of SCB-LCM on MFC has the ability to rival the NF 212, but it still has the disadvantage of lower stability. Table 2 gives the complete findings of the polarization analysis parameters Rint, MPD, the current density at MPD, the voltage at MPD, and OCV.

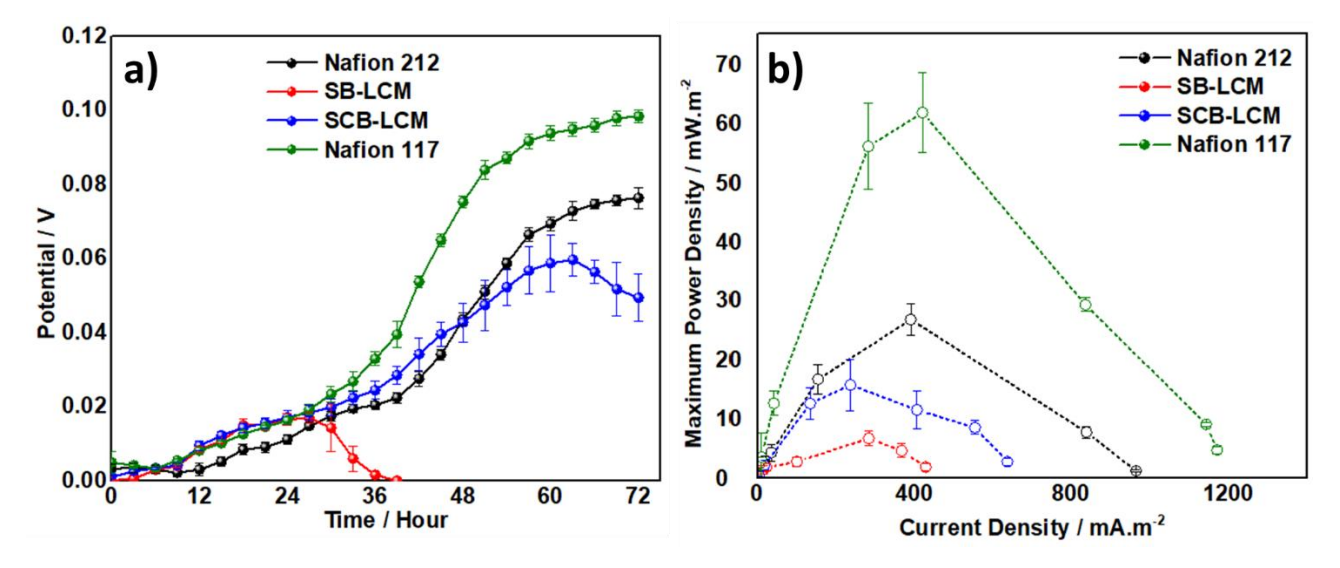


Fig. 6 a) Potential and b) power curves of MFC adopting commercial and synthesized membrane as separator

Table 2MPD, current density at MPD, voltage at MPD, and OCV of MFC adopting commercial and synthesized membrane as separator

| Parameters | Nafion 212 | Nafion 117 | SB-LCM | SCB-LCM |
|--------------------------------|-------------------|-------------------|-------------------|-------------------|
| MPD (mW/m²) | 26.84 ± 2.73 | 61.74 ± 6.73 | 6.77 ± 1.24 | 15.77 ± 4.34 |
| Current density at MPD (mA/m²) | 390.71 | 420 | 283.93 | 237.36 |
| Voltage at MPD (V) | 0.069 ± 0.011 | 0.147 ± 0.035 | 0.024 ± 0.003 | 0.066 ± 0.035 |
| OCV (V) | 0.327 ± 0.010 | 0.560 ± 0.020 | 0.203± 0.021 | 0.223 ± 0.020 |

SCB-LCM might exhibit superior ionic conductivity in comparison to SB-LCM. This heightened ionic conductivity promotes more efficient proton transport and electron transfer between the anode and cathode, resulting in increased power generation. The swelling behavior of the membrane is crucial in MFCs, as excessive swelling can lead to a decrease in ion transport and membrane stability. SCB-LCM may exhibit more controlled swelling behavior, maintaining a stable proton exchange environment and optimizing power generation. The unique combination of starch and carrageenan in SCB-LCM could lead to synergistic interactions that enhance its properties, resulting in higher power densities.

3.5 Techno-Economy analysis (TEA)

It is important to analyze the data from the Table 3 to understand the techno-economic aspects of the four membranes: Nafion 212, Nafion 117, SB-LCM, and SCB-LCM. Regarding cost, SB-LCM and SCB-LCM stand out as the most cost-effective options with costs of \$0.34/g and \$0.44/g, respectively. On the other hand, Nafion 212 and Nafion 117 are more expensive, with costs of \$10.83/m² and \$20/m², respectively. The lower costs of SB-LCM and SCB-LCM suggest potential advantages for large-scale applications where cost reduction is crucial. The cost variations stem from the differences in raw material prices and the manufacturing processes of the membranes. Nafion membranes, being wellestablished and commercially available, often come with a higher price tag due to their production complexity and demand in various industries. SB-LCM and SCB-LCM, being relatively newer and less commonly used, might benefit from lower material costs and simplified production methods, resulting in more cost-effective options. The ratio of power-to-cost provides insights into the cost-effectiveness of power generation for each membrane. SB-LCM shows the highest power-to-cost ratio at 19.91 mW/m².USD, followed by SCB-LCM at 35.84 mW/m².USD. Nafion 212 and Nafion 117 demonstrate lower power-to-cost ratios of 2.48 mW/m2.USD and 3.09

mW/m².USD, respectively. The power-to-cost ratio highlights the balance between power generation capability and the associated cost. Nafion membranes, while efficient in power generation, might not be the most cost-effective option, as the relatively higher costs reduce the power-to-cost ratio. On the other hand, SB-LCM and SCB-LCM, with lower costs, demonstrate a more favorable power-to-cost ratio, making them attractive candidates for cost-sensitive applications. Conversely, the cost-to-power ratio quantifies the cost required to generate one mW of power. SB-LCM and SCB-LCM offer the best cost-to-power ratios, requiring only 0.05 USD.m²/mW and 0.03 USD.m²/mW, respectively. Nafion 117 and Nafion 212 have higher cost-to-power ratios of 0.32 USD.m²/mW and 0.40 USD.m²/mW, respectively. The cost-to-power ratio emphasizes the economic efficiency of power generation. SB-LCM and SCB-LCM's lower cost-to-power ratios indicate that they require less investment to produce one mW of power compared to Nafion membranes. When considering the electrode area of 0.0007 m², the calculated cost-to-power ratios for SB-LCM and SCB-LCM are 71.43 and 42.86 USD/mW, respectively. Notably, these values significantly contrast with the findings of Wu et al. (2021), whose research on immobilized microalgae-based MFCs reported cost-to-power ratios as high as 490.46 USD/mW. This comparison underscores the markedly lower cost implications associated with our studied membranes, providing a distinct economic advantage in the context of microbial fuel cell technologies. This cost advantage makes SB-LCM and SCB-LCM economically attractive for large-scale applications where reducing the cost per unit of power generated is crucial.

The TEA reveals a trade-off between power generation efficiency and cost-effectiveness. Nafion membranes offer high power generation efficiency but may not be the most economical choice, especially in applications that demand large membrane surface areas or volumes. On the other hand, SB-LCM and SCB-LCM offer cost-effective options with acceptable power generation capabilities, making them suitable for

Table 3Ratio power-to-cost and ratio cost-to-power of MFC which adopting commercial and synthesized membrane as separator

| Membrane Type | MPD (mW/m²) | Cost* (USD) | Ratio power-to-cost | Ratio cost-to-power | |
|---------------|-----------------|----------------|---------------------|---------------------|--|
| Membrane Type | MFD (IIIW/III) | Cost (O3D) | $(mW/m^2.USD)$ | $(USD.m^2/mW)$ | |
| Nafion 212 | 26.84 | 10.83ª | 2.48 | 0.40 | |
| Nafion 117 | 61.74 | 20ª | 3.09 | 0.32 | |
| SB-LCM | 6.77 | $0.34^{\rm b}$ | 19.91 | 0.05 | |
| SCB-LCM | 15.77 | $0.44^{\rm b}$ | 35.84 | 0.03 | |

^{*}Membrane cost only for 25 cm²

a based-on sigma Aldrich price and then adjusted based on area of 25 cm2

^b based-on local market price

applications with budget constraints or where cost efficiency is a priority.

4. Conclusion

This study aimed to address the issues associated with costly and environmentally harmful membranes used in MFCs. The main objective was to create an affordable alternative membrane by developing a blend of starch and carrageenan, known as SCB-LCM. The dominant concerns related to commercially accessible membranes, such as Nafion, which include their excessively high prices, limited sustainability, and negative environmental impacts, have prompted the need to investigate more economically and environmentally feasible substitutes. The rigorous synthesis and characterization techniques used in the development of the SCB-LCM membrane produced remarkable outcomes. The membrane demonstrated an exceptional dehydration rate of 98.87% over a span of six hours, exceeding expectations and indicating its effectiveness in resolving water management issues in the MFC system. In addition, the examination of the surface using SEM revealed a smooth shape without any pores, indicating that the membrane has good integrity and performance. The SCB-LCM membrane was shown to be superior than existing membranes, such as Nafion 117 and Nafion 212, via comparative tests. The SCB-LCM membrane demonstrated superior endurance by demonstrating little weight loss throughout a 25-hour testing period, highlighting its resilience and long-term stability in MFC applications. In addition, the MFCs that used the SCB-LCM membrane demonstrated a very competitive maximum power density of 15.77 ± 4.34 mW/m², placing it in a favorable position compared to commercially available alternatives. In addition to performance measurements, the economic feasibility of the SCB-LCM membrane was a crucial part of its evaluation. The cost-to-power ratio for MFCs using SCB-LCM was determined to be 0.03 USD.m²/mW, demonstrating its cost-effectiveness compared to Nafion. This discovery has important implications for the wider implementation of MFC technologies, because economic factors frequently determine whether they are feasible and can be scaled up. To summarize, the suggested SCB-LCM membrane proved to be a versatile solution, effectively resolving the noted issues linked to traditional membranes. The impressive performance parameters of SCB-LCM, including dehydration rate, surface morphology, durability, and power production, make it a potential, costeffective, and environmentally friendly alternative to Nafion in the field of MFC applications. These results highlight the effectiveness of the present work and provide a strong basis for future research efforts to advance sustainable membrane technology in MFCs and related sectors.

Acknowledgments

The authors thanks to Center of Biomass and Renewable Energy and also Bioelectrochemistry Research Group – Diponegoro University for providing research facilities.

Author Contributions: M.C.: Conceptualization, methodology, formal analysis, writing—original draft, supervision, resources, project administration, S.K.; writing—review and editing, validation, A.A.S.: writing—review and editing, validation. H.H: Writing; editing. All authors have read and agreed to the published version of the manuscript.

Funding: The author(s) received no financial support for the research, authorship, and/or publication of this article.

Conflicts of Interest: The authors declare no conflict of interest.

References

- Abdou, E. S., & Sorour, M. A. (2014). Preparation and characterization of starch/carrageenan edible films. *International Food Research Journal*, 21(1), 189–193. http://www.ifrj.upm.edu.my/21%20(01)%202014/27%20IFRJ%2021%20(01)%202014%20Manal%20348.pdf
- Ahmed, A., Niazi, M. B. K., Jahan, Z., Samin, G., Pervaiz, E., Hussain, A., & Mehran, M. T. (2020). Enhancing the thermal, mechanical and swelling properties of PVA/starch nanocomposite membranes incorporating gC 3 N 4. *Journal of Polymers and the Environment, 28*, 100-115. https://doi.org/10.1007/s10924-019-01592-y
- Ahmed, E. M. (2015). Hydrogel: Preparation, characterization, and applications: A review. *Journal of Advanced Research*, 6(2), 105–121. https://doi.org/10.1016/j.jare.2013.07.006
- Arun, J., SundarRajan, P., Pavithra, K. G., Priyadharsini, P., Shyam, S., Goutham, R., ... & Pugazhendhi, A. (2024). New insights into microbial electrolysis cells (MEC) and microbial fuel cells (MFC) for simultaneous wastewater treatment and green fuel (hydrogen) generation. *Fuel*, 355, 129530. https://doi.org/10.1016/j.fuel.2023.129530
- Ayyaru, S., & Dharmalingam, S. (2011). Development of MFC using sulphonated polyether ether ketone (SPEEK) membrane for electricity generation from waste water. *Bioresource Technology*, 102(24), 11167–11171. https://doi.org/10.1016/j.biortech.2011.09.021
- Boas, J. V., Oliveira, V. B., Simões, M., & Pinto, A. M. (2022). Review on microbial fuel cells applications, developments and costs. *Journal of Environmental Management, 307*, 114525. https://doi.org/10.1016/j.jenvman.2022.114525
- Castaño, J., Guadarrama-Lezama, A. Y., Hernández, J., Colín-Cruz, M., Muñoz, M., & Castillo, S. (2017). Preparation, characterization and antifungal properties of polysaccharide–polysaccharide and polysaccharide–protein films. *Journal of Materials Science*, 52(1), 353–366. https://doi.org/10.1007/s10853-016-0336-3
- Castaño, J., Rodríguez-Llamazares, S., Contreras, K., Carrasco, C., Pozo, C., Bouza, R., Franco, C. M. L., & Giraldo, D. (2014). Horse chestnut (Aesculus hippocastanum L.) starch: Basic physicochemical characteristics and use as thermoplastic material. Carbohydrate Polymers, 112, 677–685. https://doi.org/10.1016/j.carbpol.2014.06.046
- Chakraborty, I., Das, S., Dubey, B. K., & Ghangrekar, M. M. (2020). Novel low cost proton exchange membrane made from sulphonated biochar for application in microbial fuel cells. *Materials Chemistry and Physics*, 239, 122025. https://doi.org/10.1016/j.matchemphys.2019.122025
- Cheng, S., Ye, Y., Ding, W., & Pan, B. (2014). Enhancing power generation of scale-up microbial fuel cells by optimizing the leading-out terminal of anode. *Journal of Power Sources*, 248, 931–938. https://doi.org/10.1016/j.jpowsour.2013.10.014
- Christwardana, M., Ismojo, I., & Marsudi, S. (2021). Physical, Thermal Stability, and Mechanical Characteristics of New Bioplastic Elastomer from Blends Cassava and Tannia Starches as Green Material. *Molekul*, 16(1), 46. https://doi.org/10.20884/1.jm.2021.16.1.671
- Christwardana, M., Ismojo, I., & Marsudi, S. (2022). Biodegradation Kinetic Study of Cassava & Displayed Bioplastics as Green Material in Various Media. *Molekul*, 17(1), 19. https://doi.org/10.20884/1.jm.2022.17.1.5591
- Christwardana, M., Joelianingsih, J., Yoshi, L. A., & Hadiyanto, H. (2022). Binderless carbon nanotube/carbon felt anode to improve yeast microbial fuel cell performance. *Current Research in Green and Sustainable Chemistry*, 5, 100323. https://doi.org/10.1016/j.crgsc.2022.100323
- Cui, C., Ji, N., Wang, Y., Xiong, L., & Sun, Q. (2021). Bioactive and intelligent starch-based films: A review. *Trends in Food Science & Technology*, 116, 854–869. https://doi.org/10.1016/j.tifs.2021.08.024

- Diawara, B., Fatyeyeva, K., Ortiz, J., & Marais, S. (2021).

 Polycarbonate/mica extrusion using mixing elements:

 Improvement of transparency and thermal, mechanical and water and gas barrier properties. *Polymer*, 230, 124030.

 https://doi.org/10.1016/j.polymer.2021.124030
- Do, M. H., Ngo, H. H., Guo, W. S., Liu, Y., Chang, S. W., Nguyen, D. D., Nghiem, L. D., & Ni, B. J. (2018). Challenges in the application of microbial fuel cells to wastewater treatment and energy production: A mini review. *Science of The Total Environment*, 639, 910–920. https://doi.org/10.1016/j.scitotenv.2018.05.136
- Galus, S., & Kadzińska, J. (2016). Whey protein edible films modified with almond and walnut oils. Food Hydrocolloids, 52, 78–86. https://doi.org/10.1016/j.foodhyd.2015.06.013
- Gao, L., Luo, H., Wang, Q., Hu, G., & Xiong, Y. (2021). Synergistic Effect of Hydrogen Bonds and Chemical Bonds to Construct a Starch-Based Water-Absorbing/Retaining Hydrogel Composite Reinforced with Cellulose and Poly(ethylene glycol). ACS Omega, 6(50), 35039–35049. https://doi.org/10.1021/acsomega.1c05614
- Ghasemi, M., & Rezk, H. (2024). Performance improvement of microbial fuel cell using experimental investigation and fuzzy modelling. *Energy*, 286, 129486. https://doi.org/10.1016/j.energy.2023.129486
- Guo Kun, G. K., Hassett, D. J., & Gu, T. Y. (2012). Microbial fuel cells: electricity generation from organic wastes by microbes. In Microbial biotechnology: energy and environment (pp. 162–189). CABI. https://doi.org/10.1079/9781845939564.0162
- Guo, Z., Wei, Y., Zhang, Y., Xu, Y., Zheng, L., Zhu, B., & Yao, Z. (2022).

 Carrageenan oligosaccharides: A comprehensive review of preparation, isolation, purification, structure, biological activities and applications. *Algal Research*, 61, 102593. https://doi.org/10.1016/j.algal.2021.102593
- Hadiyanto, H., Christwardana, M., Pratiwi, W.Z., Purwanto, P., Sudarno, S., Haryani, K., Hoang, A.T. (2022). Response surface optimization of microalgae microbial fuel cell (MMFC) enhanced by yeast immobilization for bioelectricity production, *Chemosphere*, 287(3), 132275. https://doi.org/10.1016/j.chemosphere.2021.132275
- Hadiyanto, H., Christwardana, M., da Costa, C. (2023) Electrogenic and biomass production capabilities of a Microalgae–Microbial fuel cell (MMFC) system using tapioca wastewater and Spirulina platensis for COD reduction. Energy Sources, Part A: Recovery, Utilization, and Environmental Effects, 45:2, 3409-3420, https://doi.org/10.1080/15567036.2019.1668085
- He, L., Du, P., Chen, Y., Lu, H., Cheng, X., Chang, B., & Wang, Z. (2017). Advances in microbial fuel cells for wastewater treatment. Renewable and Sustainable Energy Reviews, 71, 388–403. https://doi.org/10.1016/j.rser.2016.12.069
- Hernández-Fernández, F. J., Pérez de los Ríos, A., Mateo-Ramírez, F., Godínez, C., Lozano-Blanco, L. J., Moreno, J. I., & Tomás-Alonso, F. (2015). New application of supported ionic liquids membranes as proton exchange membranes in microbial fuel cell for waste water treatment. *Chemical Engineering Journal*, 279, 115–119. https://doi.org/10.1016/j.cej.2015.04.036
- Hernández-Flores, G., Poggi-Varaldo, H. M., Solorza-Feria, O., Noyola, M. T. P., Romero-Castanón, T., & Rinderknecht-Seijas, N. (2015). Improvement of Microbial Fuel Cell Performance by Selection of Anodic Materials and Enrichment of Inoculum. *Journal of New Materials for Electrochemical Systems*, 18(3), 121–129. https://doi.org/10.14447/jnmes.v18i3.357
- Hernández-Flores, G., Poggi-Varaldo, H. M., Solorza-Feria, O., Ponce-Noyola, M. T., Romero-Castañón, T., Rinderknecht-Seijas, N., & Galíndez-Mayer, J. (2015). Characteristics of a single chamber microbial fuel cell equipped with a low-cost membrane. International Journal of Hydrogen Energy, 40(48), 17380–17387. https://doi.org/10.1016/j.ijhydene.2015.10.024
- Idris, S. A., Esat, F. N., Abd Rahim, A. A., Zahin Rizzqi, W. A., Ruzlee, W., & Zyaid Razali, W. M. (2016). Electricity generation from the mud by using microbial fuel cell. *MATEC Web of Conferences*, 69, 02001. https://doi.org/10.1051/matecconf/20166902001
- Jatoi, A. S., Akhter, F., Mazari, S. A., Sabzoi, N., Aziz, S., Soomro, S. A., Mubarak, N. M., Baloch, H., Memon, A. Q., & Ahmed, S. (2021). Advanced microbial fuel cell for waste water treatment—a

- review. Environmental Science and Pollution Research, 28(5), 5005–5019. https://doi.org/10.1007/s11356-020-11691-2
- Kim, J. R., Cheng, S., Oh, S.-E., & Logan, B. E. (2007). Power Generation Using Different Cation, Anion, and Ultrafiltration Membranes in Microbial Fuel Cells. *Environmental Science & Technology*, 41(3), 1004–1009. https://doi.org/10.1021/es062202m
- Kondaveeti, S., Lee, J., Kakarla, R., Kim, H. S., & Min, B. (2014). Low-cost separators for enhanced power production and field application of microbial fuel cells (MFCs). *Electrochimica Acta*, 132, 434–440. https://doi.org/10.1016/j.electacta.2014.03.046
- Kumar, R., Singh, L., Energy, A. Z.-R. and S., & 2016, undefined. (2016). Exoelectrogens: recent advances in molecular drivers involved in extracellular electron transfer and strategies used to improve it for microbial fuel cell applications. *Elsevier*. https://doi.org/10.1016/j.rser.2015.12.029
- Kumar, R., Singh, L., Wahid, Z. A., & Din, M. F. Md. (2015). Exoelectrogens in microbial fuel cells toward bioelectricity generation: a review. *International Journal of Energy Research*, 39(8), 1048–1067. https://doi.org/10.1002/er.3305
- Maddalwar, S., Nayak, K. K., Kumar, M., & Singh, L. (2021). Plant microbial fuel cell: opportunities, challenges, and prospects. *Bioresource Technology*, 341, 125772. https://doi.org/10.1016/j.biortech.2021.125772
- Maity, J. P., Bundschuh, J., Chen, C.-Y., & Bhattacharya, P. (2014). Microalgae for third generation biofuel production, mitigation of greenhouse gas emissions and wastewater treatment: Present and future perspectives – A mini review. *Energy*, 78, 104–113. https://doi.org/10.1016/j.energy.2014.04.003
- Moharir, P. V., & Tembhurkar, A. R. (2018). Comparative performance evaluation of novel polystyrene membrane with ultrex as Proton Exchange Membranes in Microbial Fuel Cell for bioelectricity production from food waste. *Bioresource Technology*, 266, 291– 296. https://doi.org/10.1016/j.biortech.2018.06.085
- Mohr, S., Wang, J., Ward, J., & Giurco, D. (2021). Projecting the global impact of fossil fuel production from the Former Soviet Union. *International Journal of Coal Science & Technology*, 8(6), 1208-1226. https://doi.org/10.1007/s40789-021-00449-x
- Obileke, K., Onyeaka, H., Meyer, E. L., & Nwokolo, N. (2021). Microbial fuel cells, a renewable energy technology for bio-electricity generation: A mini-review. *Electrochemistry Communications*, *125*, 107003. https://doi.org/10.1016/j.elecom.2021.107003
- Oh, S.-E., & Logan, B. E. (2006). Proton exchange membrane and electrode surface areas as factors that affect power generation in microbial fuel cells. *Applied Microbiology and Biotechnology*, 70(2), 162–169. https://doi.org/10.1007/s00253-005-0066-y
- Pant, D., Singh, A., Van Bogaert, G., Irving Olsen, S., Singh Nigam, P., Diels, L., & Vanbroekhoven, K. (2012). Bioelectrochemical systems (BES) for sustainable energy production and product recovery from organic wastes and industrial wastewaters. *RSC* Adv., 2(4), 1248–1263. https://doi.org/10.1039/C1RA00839K
- Paucar, N. E., & Sato, C. (2021). Microbial Fuel Cell for Energy Production, Nutrient Removal and Recovery from Wastewater: A Review. *Processes*, 9(8), 1318. https://doi.org/10.3390/pr9081318
- Qureshi, D., Nayak, S. K., Maji, S., Kim, D., Banerjee, I., & Pal, K. (2019).

 Carrageenan: A Wonder Polymer from Marine Algae for Potential Drug Delivery Applications. *Current Pharmaceutical Design*, 25(11), 1172–1186. https://doi.org/10.2174/1381612825666190425190754
- Rabaey, K., & Verstraete, W. (2005). Microbial fuel cells: novel biotechnology for energy generation. *Trends in Biotechnology*, 23(6), 291–298. https://doi.org/10.1016/j.tibtech.2005.04.008
- Sandhu, K. S., Sharma, L., Kaur, M., & Kaur, R. (2020). Physical, structural and thermal properties of composite edible films prepared from pearl millet starch and carrageenan gum: Process optimization using response surface methodology. *International Journal of Biological Macromolecules*, 143, 704–713. https://doi.org/10.1016/j.ijbiomac.2019.09.111
- Senthilkumar, K., Anappara, S., Krishnan, H., & Ramasamy, P. (2020).

 Simultaneous power generation and Congo red dye degradation in double chamber microbial fuel cell using spent carbon electrodes. Energy Sources, Part A: Recovery, Utilization, and Environmental Effects, 1–17. https://doi.org/10.1080/15567036.2020.1781978

- Shabani, M., Younesi, H., Pontié, M., Rahimpour, A., Rahimnejad, M., & Zinatizadeh, A. A. (2020). A critical review on recent proton exchange membranes applied in microbial fuel cells for renewable energy recovery. *Journal of cleaner production, 264*, 121446. https://doi.org/10.1016/j.jclepro.2020.121446
- Shrgawi, N., Shamsudin, I. J., Hanibah, H., Kasim, N., Noor, S. A. M., & Taufik, S. (2023). Green electrolyte host based on synthesized benzoyl kappa-carrageenan: Reduced hydrophilicity and improved conductivity. *Arabian Journal of Chemistry*, *16*(5), 104687. https://doi.org/10.1016/j.arabjc.2023.104687
- Singla, M. K., Nijhawan, P., & Oberoi, A. S. (2021). Hydrogen fuel and fuel cell technology for cleaner future: a review. *Environmental Science and Pollution Research*, 28, 15607-15626. https://doi.org/10.1007/s11356-020-12231-8
- Sirajudeen, A. A. O., Annuar, M. S. M., Ishak, K. A., Yusuf, H., & Subramaniam, R. (2021). Innovative application of biopolymer composite as proton exchange membrane in microbial fuel cell utilizing real wastewater for electricity generation. *Journal of Cleaner Production*, 278, 123449. https://doi.org/10.1016/j.jclepro.2020.123449
- Sonawane, J. M., Pant, D., Ghosh, P. C., & Adeloju, S. B. (2019). Fabrication of a Carbon Paper/Polyaniline-Copper Hybrid and Its Utilization as an Air Cathode for Microbial Fuel Cells. *ACS Applied Energy Materials*, *2*(3), 1891–1902. https://doi.org/10.1021/acsaem.8b02017
- Tebaldi, C., Ranasinghe, R., Vousdoukas, M., Rasmussen, D. J., Vega-Westhoff, B., Kirezci, E., ... & Mentaschi, L. (2021). Extreme sea levels at different global warming levels. *Nature Climate Change*, 11, 746-751. https://doi.org/10.1038/s41558-021-01127-1
- Tse, T. J., Wiens, D. J., & Reaney, M. J. (2021). Production of bioethanol—A review of factors affecting ethanol yield. Fermentation, 7(4), 268. https://doi.org/10.3390/fermentation7040268
- Vishwanathan, A. S. (2021). Microbial fuel cells: a comprehensive review for beginners. *3 Biotech*, *11*(5), 248. https://doi.org/10.1007/s13205-021-02802-y
- Wang, Y., Li, B., Cui, D., Xiang, X., & Li, W. (2014). Nano-molybdenum carbide/carbon nanotubes composite as bifunctional anode catalyst for high-performance Escherichia coli-based microbial fuel cell. *Biosensors and Bioelectronics*, *51*, 349–355. https://doi.org/10.1016/j.bios.2013.07.069
- Winfield, J., Gajda, I., Greenman, J., & Ieropoulos, I. (2016). A review into the use of ceramics in microbial fuel cells. *Bioresource Technology*, 215, 296–303. https://doi.org/10.1016/j.biortech.2016.03.135
- Wu, J. Y., Lay, C. H., Chia, S. R., Chew, K. W., Show, P. L., Hsieh, P. H., & Chen, C. C. (2021). Economic potential of bioremediation using immobilized microalgae-based microbial fuel cells. *Clean Technologies and Environmental Policy*, 23, 2251-2264. https://doi.org/10.1007/s10098-021-02131-x

- Xia, X., Tokash, J. C., Zhang, F., Liang, P., Huang, X., & Logan, B. E. (2013). Oxygen-Reducing Biocathodes Operating with Passive Oxygen Transfer in Microbial Fuel Cells. *Environmental Science & Technology*, 47(4), 2085–2091. https://doi.org/10.1021/es3027659
- Xu, X., Zhao, Q., Wu, M., Ding, J., & Zhang, W. (2017). Biodegradation of organic matter and anodic microbial communities analysis in sediment microbial fuel cells with/without Fe(III) oxide addition. Bioresource Technology, 225, 402–408. https://doi.org/10.1016/j.biortech.2016.11.126
- Yadav, S., Ibrar, I., Altaee, A., Samal, A. K., & Zhou, J. (2022). Surface modification of nanofiltration membrane with kappacarrageenan/graphene oxide for leachate wastewater treatment. *Journal of Membrane Science*, 659, 120776. https://doi.org/10.1016/j.memsci.2022.120776
- Yang, Z., Pei, H., Hou, Q., Jiang, L., Zhang, L., & Nie, C. (2018). Algal biofilm-assisted microbial fuel cell to enhance domestic wastewater treatment: Nutrient, organics removal and bioenergy production. *Chemical Engineering Journal*, 332, 277–285. https://doi.org/10.1016/j.cej.2017.09.096
- Yu, Y.-Y., Guo, C. X., Yong, Y.-C., Li, C. M., & Song, H. (2015). Nitrogen doped carbon nanoparticles enhanced extracellular electron transfer for high-performance microbial fuel cells anode. Chemosphere, 140, 26–33. https://doi.org/10.1016/j.chemosphere.2014.09.070
- Zhang, L., Wang, J., Fu, G., & Zhang, Z. (2020). Simultaneous electricity generation and nitrogen and carbon removal in single-chamber microbial fuel cell for high-salinity wastewater treatment. *Journal of Cleaner Production*, 276, 123203. https://doi.org/10.1016/j.jclepro.2020.123203
- Zhang, Y., Liu, M., Zhou, M., Yang, H., ... L. L., & 2019, undefined. (2019). Microbial fuel cell hybrid systems for wastewater treatment and bioenergy production: synergistic effects, mechanisms and challenges. *Elsevier*, 103, 13–29. https://www.sciencedirect.com/science/article/pii/S1364032 118308220
- Zhong, Y., Godwin, P., Jin, Y., & Xiao, H. (2020). Biodegradable polymers and green-based antimicrobial packaging materials: A mini-review. *Advanced Industrial and Engineering Polymer Research*, 3(1), 27–35. https://doi.org/10.1016/j.aiepr.2019.11.002
- Zhuang, L., Zhou, S., Wang, Y., Liu, C., & Geng, S. (2009). Membrane-less cloth cathode assembly (CCA) for scalable microbial fuel cells. *Biosensors and Bioelectronics*, 24(12), 3652–3656. https://doi.org/10.1016/j.bios.2009.05.032



© 2024. The Author(s). This article is an open access article distributed under the terms and conditions of the Creative Commons Attribution-ShareAlike 4.0 (CC BY-SA) International License (http://creativecommons.org/licenses/by-sa/4.0/)